SMART-COMMIT and MODIS Deep Blue Measurements of Airborne Saharan Dust during the NAMMA Field Experiment

M.-J. Jeong[1,2], Q. Ji[2,3], S.-C. Tsay[2], N.C. Hsu[2], R.A. Hansell[2,3], J. Lee[2,3], and S. Bell[2,4]

[1]Goddard Earth Sciences and Technology Center, University of Maryland Baltimore County, Baltimore, MD.

[2]Goddard Space Flight Center, National Aeronautics and Space Administration, Greenbelt, MD.

[3]Earth System Science Interdisciplinary Center, University of Maryland, College Park, MD.

[4]Science Systems and Applications Inc., Lanham, MD.

1. Introduction

❖ Uncertainties in optical properties of mineral dust pose large uncertainties in its impact on the climate system (Forster et al, 2007).

❖ Absorption by dust originating from different source regions has not yet been represented by global models (Forster et al, 2007).

❖ It is very difficult to measure transported dust from the surface as dust particles are mixed with boundary layer aerosols.

❖ NASA's two mobile laboratories, Surface-sensing Measurements for Atmospheric Radiative Transfer (SMART) and Chemical, Optical, and Microphysical Measurements of In-situ Troposphere (COMMIT) were deployed at Sal island, Cape Verde, during Sep 2 ~ Sep 28, 2006 as a part of NASA African Monsoon Multidisciplinary Activities (NAMMA). Among a suite of instruments aboard the SMART-COMMIT, data from Micro-Pulse Lidar, TSI Nephelometer, Radiance Research Nephelometers, and Particle/Soot Absorption Photometer are used to derive the optical properties of the transported airborne mineral dust from the Saharan desert. A comprehensive look on the selected dust episodes by SMART-COMMIT together with back-trajectory and MODIS *Deep Blue* aerosol products is provided to better characterize airborne Saharan dust.

2. Derivation of Dust Optical Property

Suppose an aerosol layer is a mixture of two hypothetical components – "Dust" and "Background" aerosols. The measured scattering coefficients become the sum of those two components:

$$k_{sca,Mix}(RH) = k_{sca,Bg}(RH) + k_{sca,Du}(RH)$$

Scattering coefficients, mass scattering efficiency, and dry mass concentration for aerosols bear the following relationship:

$$\sigma^m_{sca}(RH) = \frac{k_{sca}(RH)}{M^d}$$

Aerosol humidification factor, f(RH), is defined as follows:

$$f(RH) \equiv \frac{k_{sca}(RH\%)}{k_{sca}(40\%)}$$

By manipulating the equations above, a parameter, γ, can be defined as:

$$\gamma \equiv \frac{k_{sca,Du}(40\%)}{k_{sca,Bg}(40\%)} = \frac{f_{Bg}(85\%) - f_{Mix}(85\%)}{f_{Mix}(85\%) - f_{Du}(85\%)}$$

Thus, the scattering coefficients for "Dust" and "Background" aerosols are

$$k_{sca,Du}(40\%) = \frac{\gamma}{\gamma+1} k_{sca,Mix}(40\%)$$

$$k_{sca,Bg}(40\%) = \frac{1}{\gamma+1} k_{sca,Mix}(40\%)$$

Finally, mass concentration, mass scattering efficiency, and single scattering albedo for "Dust" can be derived as follows:

$$M^d_{Du} = M^d_{Mix} - \frac{1}{\sigma^m_{Bg}(40\%)\cdot(\gamma+1)} k_{sca,Mix}(40\%)$$

$$\sigma^m_{sca,Du} = \frac{\gamma}{M^d_{Du}(\gamma+1)} k_{sca,Mix}(40\%)$$

$$\omega_{Du} = \frac{1}{\gamma}\left[(1+\gamma)\omega_{Mix} - \omega_{Bg}\right]$$

The following parameters need to be considered as *a priori* in order to derive dust optical properties using the equations above:
1) mass scattering coefficients of "Background" aerosols;
2) aerosol humidification factor (AHF) of "Background" aerosols;
3) single scattering albedo (SSA) of "Background" aerosols; and
4) AHF for "Dust" aerosols.
The former three are determined from measurements during the experiment (1.54 [±0.19] m^2 g^{-1}, 2.5 [±0.05], and 0.995 [±0.005], respectively) and AHF for dust is assumed to be 1.1 (e.g., Anderson et al., 2003)

3. Dust Episodes

Several dust episodes were identified and captured by the SMART-COMMIT mobile laboratories during the 2006 NAMMA experiment. Two episodes were chosen as cases for further analysis: "Case I" for the episode during Sep 11~13, 2006 and "Case II" for the episode during Sep 19~20, 2006.

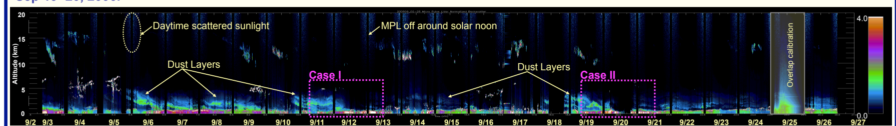

Fig 1. Time series of normalized back-scatter profiles measured from Micro-Pulse Lidar at Sal, Cape Verde during Sep 2 ~ Sep 26, 2006.

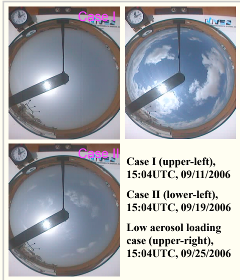

Fig 2. Whole sky images observed at the surface for the two dusty cases and a case with low aerosol loading.

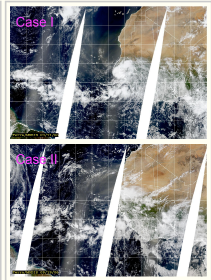

Fig 3. RGB images taken from MODIS/Terra for the two dust cases.

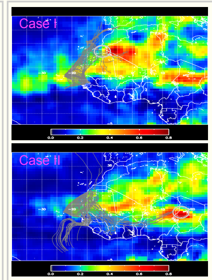

Fig 4. MODIS *Deep Blue* AOT averaged for 7 days on and prior to the beginning of each case. The superimposed gray lines are 7-day back-trajectories terminating at Sal, Cape Verde (16.7N, 22.9W). Each line represents a back-trajectory ending at every hour throughout the period of each case.

Areas with high AOT indicate the location and the loading of mineral dust during each respective period. Combined with the back-trajectories, source regions for dust measured in situ at Sal, Cape Verde can be inferred. It is obvious that dust measured at the surface originated from different sources between the two cases.

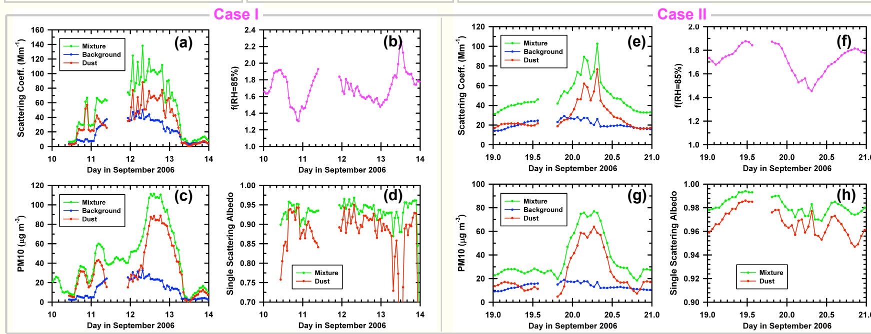

Fig 5. (a) Scattering coefficients for Mixture, Background, and Dust aerosols during Sep 10~13. (b) Aerosol scattering humidification factor, f(RH), defined at RH=85% during Sep 10~13. (c) Mass concentration (PM10) for Mixture, Background, and Dust aerosols during Sep 10~13. (d) Single scattering albedo for Mixture and Dust aerosols (0.55μm) during Sep 10~13. (e) Same as Fig 5a, but during Sep 19~20. (f) Same as Fig 5b, but during Sep 19~20. (g) Same as Fig 5c, but during Sep 19~20. (h) Same as Fig 5d, but during Sep 19~20.

4. Summary of the Derived Dust Optical Property

Table 1. Mean and standard deviation (Std.) of the derived mass scattering efficiency and single scattering albedo for the dust cases in this study.

Parameter	Case I		Case II	
	$\sigma_{sca,Du}(40\%)$ [m^2 g^{-1}]	ω_{Du}(0.55μm)	$\sigma_{sca,Du}(40\%)$ [m^2 g^{-1}]	ω_{Du} (0.55μm)
Mean (±Std.)	1.21 (±0.71)	0.900 (±0.049)	0.93 (±0.17)	0.961 (±0.012)

5. Sensitivity Test

Sensitivities of the derived quantities (i.e., mass scattering efficiency and single scattering albedo for dust) to input parameters are examined by posing relative errors in the input parameters.

Table 3. Sensitivity of the derived "Dust Mass Scattering Efficiency" to the relative errors in "Background f(85%)" and "Background σ_{sca} (40%)" [Unit: %].

Input Parameters	Relative Errors in the Input Parameters					
	-20%	-10%	-5%	+5%	+10%	+20%
f_{Bg}(85%)	9.9	5.3	1.0	-0.4	-0.8	-1.6
$\sigma_{sca,Bg}$(40%)	41.5	11.9	5.1	-4.0	-7.3	-12.4

Table 4. Sensitivity of the derived "Dust Single Scattering Albedo (SSA)" to the relative errors in "Background f(85%)" [Unit: %].

Input Parameter	Relative Errors in the Input Parameters					
	-20%	-10%	-5%	+5%	+10%	+20%
f_{Bg}(85%)	-3.2	-1.0	-0.5	0.3	0.7	0.9

6. Discussion

Aerosol Direct Radiative Effects in Visible (400-700nm)

Input Aerosol Models
• Size distributions and refractive indices were constructed from the AERONET inversion product (September, 2001-2005)
• Spectral dependency of aerosol extinction coefficients & asymmetry parameter from Mie calculation based on the size distribution and refractive indices from the AERONET inversion product
• Dust single scattering albedo derived for Case I & II from in-situ measurements

Differences in direct aerosol radiative effects (ADRE) between the two cases (SZA=45º, τ=1.0).

TOA: -11.9W/m2/τ; Surface: -22.6W/m2/τ; Atmosphere: +34.5W/m2/τ

→ Significant differences in ADRE in terms of disposition of the solar energy in the earth-atmosphere system are expected unless the optical properties of dust transported from varied source regions are considered properly.

7. Summary and Suggestion

❖ A new method was developed to derive the mass scattering efficiency and single scattering albedo for dust from a suite of surface in-situ measurements.

❖ Several transported Saharan dust episodes were identified in which dust layers descended down to the surface.

❖ Significant differences in mass scattering efficiency and single scattering albedo were found for two selected cases.

❖ Back-trajectory analysis suggests that the dust for the two cases were transported from different source regions.

❖ Significant differences in ADRE between the two dust cases suggest that transport models need to include source-region-dependent dust optical properties for better assessments for ADRE.

Table 2. AOT (550nm) and SSA (412nm) from Deep Blue aerosol product for the areas encompassed by light gray circles in Fig 4 for respective cases.

	Case I	Case II
Deep Blue AOT	1.381 (±0.270)	2.833 (±0.769)
Deep Blue SSA	0.915 (±0.004)	0.959 (±0.011)